THE JOURNAL OF PHYSICAL CHEMISTRY B
A JOURNAL OF THE AMERICAN CHEMICAL SOCIETY

pubs.acs.org/JPCB

Article

# Excluded-Volume Interactions in Field-Theoretic Simulations: Multiconvolutions and Model Equivalence

Alexander Weyman* and Vlasis G. Mavrantzas*

Cite This: J. Phys. Chem. B 2022, 126, 10948−10954

Read Online

ACCESS | Metrics & More | Article Recommendations

**ABSTRACT:** To deal with divergences of functional integrals in field-theoretic simulations (FTS) of complex fluids, the microscopic density is often smeared by being replaced by a convoluted one, typically using a Gaussian masking function. The smearing changes radically the nature of nonbonded interactions of the original microscopic density and results in a regularized model that is free of ultraviolet (UV) divergences. In this work, we first resolve a few fundamental issues related with the use of masking functions for $\delta$-interactions in FTS and then we detail a new methodology that builds on the concept of multiconvoluted inverse potentials and a principle of model equivalence for statistical weights to accommodate more physically relevant interactions in FTS. The capabilities of the new approach are highlighted by examining the Gaussian-regularized Edwards model (GREM) and the Yukawa potential. A successful test calculation of the excess chemical potential of a polymer chain in a good solvent with the GREM illustrates the power of the new theoretical framework.

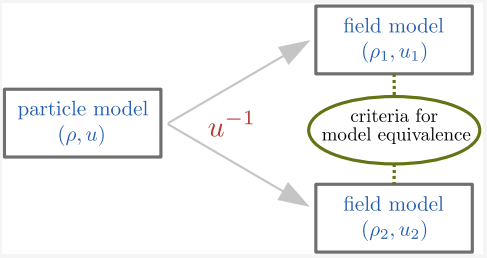


## 1. INTRODUCTION

In a series of papers in 1965 and 1966, Edwards[1,2] proposed a theory for homopolymer chains in good solvent based on a minimal model for pairwise, excluded-volume interactions in the form of a Dirac delta function, $u(\mathbf{r} - \mathbf{r}') = u_0\, \delta(\mathbf{r} - \mathbf{r}')$, with $u_0$ being the strength parameter of the interaction. As noted by Villet and Fredrickson,[3] despite its simplicity, such a purely repulsive model has served over the years as a prototype for more complicated field theories. For example, in conjunction with the continuous Gaussian chain backbone, the model has helped capture many universal features of polymer solutions.[4−7] Edwards had also noted that a field theory based on such a treatment of nonbonded interactions exhibits an ultraviolet (UV) divergence originating from infinite functional integrals involving polymer-segment self-interaction energies. To control this divergence, Villet and Fredrickson proposed a regularization framework that replaces the Dirac delta with a Gaussian interaction potential that is finite on contact. Following Wang's[8] regularization scheme for electrolyte solutions, they treated polymer monomers not as point masses but as the centers of a Gaussian density distribution. It is this distributed mass that interacts then by a delta function potential, thus overcoming the pathologies of the original model. Villet and Fredrickson used a Gaussian form for the masking function

$$\Gamma(\mathbf{r}) = \frac{1}{(2\pi a^2)^{3/2}} \exp\left(-\frac{|\mathbf{r}|^2}{2a^2}\right) \tag{1}$$

where $a$ describes a characteristic polymer-segment (e.g., a monomer) length scale. This is known today as the Gaussian-regularized Edwards model (GREM). Prakash and Öttinger[9] have also used a narrow Gaussian repulsive potential to regularize excluded-volume effects described by a $\delta$-function in Brownian dynamics simulations of dilute polymer solutions. We also mention the treatment of nonbonded interactions in the form of a weighted density functional, which has been used to regularize microscopic particle densities in the context of self-consistent mean-field calculations.[10−13]

Mathematically, the new mass density field $\breve{\rho}(\mathbf{r})$ is defined by the convolution of the masking (or distribution) function with the monomer position density $\hat{\rho}(\mathbf{r})$ as $\breve{\rho}(\mathbf{r}) = \int \Gamma(\mathbf{r} - \mathbf{r}')\hat{\rho}(\mathbf{r}')\, \mathrm{d}^3r'$ or, equivalently, $\breve{\rho}(\mathbf{r}) = [\Gamma * \hat{\rho}]\ (\mathbf{r})$. Due to the convoluted microscopic density, the total interaction potential between $n$ particles in volume $V$, $U[\{\mathbf{r}^n\}] = \frac{1}{2} \int_V \mathrm{d}^3r \int_V \mathrm{d}^3r' \hat{\rho}(\mathbf{r}) u(\mathbf{r} - \mathbf{r}')\hat{\rho}(\mathbf{r}') - \frac{n}{2}u(\mathbf{0})$, which is the starting point for developing the smeared version of the model, is expressed as

$$U'[\{\mathbf{r}^n\}] = \frac{1}{2} \langle \hat{\rho} | \Gamma * u * \Gamma | \hat{\rho} \rangle - \frac{n}{2} [\Gamma * u * \Gamma](\mathbf{0}) \tag{2}$$

Received: September 21, 2022
Revised: November 11, 2022
Published: December 14, 2022





https://doi.org/10.1021/acs.jpcb.2c06734
J. Phys. Chem. B 2022, 126, 10948−10954

where we have made use of Dirac's bra−ket notation.[14,15] From eq 2, we understand that the self-interaction term also involves the convolution of the masking function Γ with $u(\mathbf{0})$, thus possible model divergences arising from $u(\mathbf{0})$ can be removed. From eq 2, we also get the impression that one could have considered the entire formulation in the context of an effective potential $\Gamma * u * \Gamma$ acting on $\hat{\rho}$; however, it is important to emphasize that the particle-to-field transformation (the next step in the field-theoretic simulations, FTS model-building hierarchy) is with respect to the original pair potential $u$, i.e., it is the quantity $\Gamma * \hat{\rho}$ (namely, $\check{\rho}$) that is subjected to the transformation and not $\hat{\rho}$. In the hypothetical case of transforming with respect to the effective potential $\Gamma * u * \Gamma$ while keeping the microscopic density $\hat{\rho}$ intact, the theoretical barrier of finding the functional inverse entering the formalism through the subsequent Hubbard−Stratonovich transformation from particles to fields would have still been there. The convolution $\check{\rho} = \Gamma * \hat{\rho}$ reminds us of the unitary transformation of the wave function or of the Hamiltonian in quantum mechanics eventually resulting in a simplified form of the Schrödinger equation, which, however, has the same solution as the original problem. Moreover, in the present context, we have assumed a translationally invariant transformation, but one can also consider applying it locally by invoking a particle coarse-graining that depends on space.

Writing down the corresponding partition function in the $nVT$ ensemble ($n$ denotes the number of molecules, $V$ is the volume, and $T$ is the temperature), $\mathcal{Z}'_c \propto \int_{V^n} \mathrm{d}^{3n}r \exp(-\beta U'[\{\mathbf{r}^n\}])$, and applying the Hubbard−Stratonovich transformation, use of the Gaussian integral identity leads to

$$\mathcal{Z}'_c \propto \int_{V^n} d^{3n}r \int \mathcal{D}w \exp\left(-\frac{1}{2\beta}\langle w|u^{-1}|w\rangle - i\langle w|\Gamma * \hat{\rho}\rangle\right) \tag{3}$$

By exchanging terms in the convolution of the exponent according to $\langle w|\Gamma * \hat{\rho}\rangle = \langle \Gamma * w|\hat{\rho}\rangle$ and simplifying, we derive the following expression for the Hamiltonian of the smeared model

$$\mathcal{H}'[w] = \frac{1}{2\beta}\langle w|u^{-1}|w\rangle - n \ln Q[i\Gamma * w] \tag{4}$$

Compared to the original nonsmeared model described by

$$\mathcal{H}[w] = \frac{1}{2\beta}\langle w|u^{-1}|w\rangle - n \ln Q[iw] \tag{5}$$

the masking function Γ in the smeared one enters the Hamiltonian through the reduced partition function $Q$.

Based on the above modeling scheme, Villet and coworkers[3,16] have nicely worked out a UV regularized version of the Edwards model and of the field-based observables derived from it by adopting the three-dimensional (3D) Gaussian masking function described by eq 1. For such Gaussian masked $\delta$-interactions, the effective interactions between point particles are described through (see also ref 3)

$$u'(\mathbf{r}) = u_0[\Gamma * \Gamma](\mathbf{r}) \tag{6a}$$

$$= \frac{u_0}{(4\pi a^2)^{3/2}} \exp\left(-\frac{|\mathbf{r}|^2}{4a^2}\right) \tag{6b}$$

Effectively, point-like particles in this Gaussian-smeared description interact via a potential that is also a Gaussian but characterized by an adjusted variance $2a^2$.

Koski and co-workers have also made use of masked $\delta$-interactions to model polymer nanocomposites.[17] In their case, however, and due to the finite spatial extent of the particles, the masking function was chosen to be a complementary error function, with the understanding that the expanded (mass) structures interact locally one with the other via $\delta$-interactions. Thus, in contrast to GREM, the analytical calculation of the effective interaction potential is not anymore a straightforward task. And the same is true for the inverse problem: Given the shape of the effective interaction potential (see, e.g., Figure 3 in Koski et al.[17]), identifying the mathematical form of the underlying masking function is quite challenging.

Overall, it appears that the choice of the masking function is arbitrary to some extent or, to express it differently, there seems to be some good freedom in choosing Γ. Our goal in this work is to discuss this freedom in detail and exploit it to expand as much as possible the spectrum of advanced interactions that can be incorporated into the FTS framework. Our focus is not on the distributed-density regularization of the underlying microscopic model itself but on the more rigorous statistical-mechanical treatment of the effective nonbonded interactions that emanate from it.

## 2. THEORY

**2.1. Basic Requirements for General Smeared Density Models.** Our starting point for identifying masking functions that can transform $\delta$-interactions to tractable effective potentials for use in the FTS formalism is eq 6a above, which holds for any masking function. For the subsequent analysis, we transform this equation into Fourier space and solve formally for $\hat{\Gamma}$, the Fourier transform of Γ, with the help of the convolution theorem to get

$$\hat{\Gamma}(\mathbf{k}) = \sqrt{\frac{\hat{u}'(\mathbf{k})}{u_0}} \tag{7}$$

This simple equation may seem inconspicuous, yet it has several implications regarding the choice and actual use of masking functions. First, it implies that the Fourier transform $\hat{u}'$ of the effective pair potential should exist, a rather strict requirement since it immediately excludes the vast majority of typical pair potentials (in their unregularized form) exhibiting specific divergences at $\mathbf{r} = \mathbf{0}$. Second, and this is less obvious, the Fourier integral of radially symmetric pair potentials contains only real terms. For real masking functions, the square root must be positive, and thus, with $u_0 > 0$, $\hat{u}'$ must be positive. Because of our considering real masking functions, only those qualify for adoption in FTS for which $\hat{\Gamma}$ is also positive. Third, the derived hypothetical Fourier-transformed $\hat{\Gamma}$ should be unproblematic to treat mathematically or numerically on the way back to Γ. As we will see below, this last point sets certain requirements on the large wavenumber behavior of the function $\hat{\Gamma}$ in the corresponding Fourier integral.

In view of all of these general requirements for the masking function, the task of identifying analytic forms of Γ or $u'$ for physically meaningful interactions seems challenging. Nonetheless, the details of such a generalization can be demonstrated by means of a novel example. Motivated by the use of decaying exponential interactions as already


https://doi.org/10.1021/acs.jpcb.2c06734
J. Phys. Chem. B 2022, 126, 10948−10954

discussed in ref 15, we consider in particular the effective potential

$$u_1'(\mathbf{r}) = A\,\exp(-B|\mathbf{r}|), \quad B > 0 \tag{8}$$

whose 3D-Fourier transform is

$$\hat{u}_1'(\mathbf{k}) = \frac{8\pi AB}{(|\mathbf{k}|^2 + B^2)^2} \tag{9}$$

Using eq 7 and comparing with the functional form of the Yukawa potential

$$u_Y(\mathbf{r}) = A_Y \frac{\exp(-B_Y|\mathbf{r}|)}{|\mathbf{r}|}, \quad B_Y > 0 \tag{10}$$

whose Fourier transform is

$$\hat{u}_Y(\mathbf{k}) = \frac{4\pi A_Y}{|\mathbf{k}|^2 + B_Y^2} \tag{11}$$

we can readily identify the corresponding masking function

$$\Gamma_1(\mathbf{r}) = \sqrt{\frac{AB}{2\pi u_0}}\,\frac{\exp(-B|\mathbf{r}|)}{|\mathbf{r}|} \tag{12}$$

Exponentially decaying effective interactions such as that of eq 8 between point-like particles can thus be modeled by convolution of the microscopic density with a function similar to that of the Yukawa potential. Conversely, for the effective potential

$$u_2'(\mathbf{r}) = \frac{AB}{(|\mathbf{r}|^2 + B^2)^2}, \quad B > 0 \tag{13}$$

the Fourier pairs from eqs 8 and 9 imply the following masking function:

$$\Gamma_2(\mathbf{r}) = \sqrt{\frac{A}{u_0}}\,\frac{8B}{\pi(4|\mathbf{r}|^2 + B^2)^2} \tag{14}$$

As in the case of effective Gaussian interactions, the similarity between the functional forms of the potential $u_2'$ and the masking function $\Gamma_2$ is readily apparent.

**2.2. Reformulating an Equation for $u^{-1}$.** We turn our attention now to the particle-to-field transformation wherein the inverse potential $u^{-1}$ immediately shows up. The inverse potential is formally defined through $\int_{\mathbb{R}^3} \mathrm{d}^3r'u(\mathbf{r}, \mathbf{r}')u^{-1}(\mathbf{r}', \mathbf{r}'') = \delta(\mathbf{r} - \mathbf{r}'')$, which is equivalent to

$$[u*u^{-1}](\mathbf{r}) = \delta(\mathbf{r}) \tag{15}$$

Equation 15 allows us to solve for $u^{-1}$ through Fourier transform

$$\mathcal{F}[u^{-1}](\mathbf{k}) = (\mathcal{F}[u](\mathbf{k}))^{-1} \tag{16}$$

This last relation imposes certain constraints on the functional form of $u$ for $(\mathcal{F}[u](\mathbf{k}))^{-1}$ to be a well-defined function. First, and similar to the case of the effective interaction potential $u'$ discussed in the previous section, an important condition that $u$ must possess is to have a Fourier transform. Once again, this condition excludes hard-core models with specific divergences at $\mathbf{r} = \mathbf{0}$. Second, and to avoid divergences in $\hat{u}^{-1}(\mathbf{k}) := \mathcal{F}[u^{-1}](\mathbf{k})$, it is essential that $\hat{u}(\mathbf{k}) := \mathcal{F}[u](\mathbf{k})$ has no roots and thus does not change sign as a function of $\mathbf{k}$. Interaction potentials for which such a sign change of their Fourier transform occurs are special in other respects[18] but cannot be used in the context of the FTS methodology discussed here. In light of the discrete, positive definite matrix $\mathbf{u}$ introduced and discussed in ref 15, the typical requirement $\hat{u} > 0$ in the FTS literature[4] is then rather straightforward to understand.

Equation 16 reveals a key theoretical problem in the relation between $u$ and $u^{-1}$: Typical interaction potentials $u$, such as the Yukawa one discussed above, drop to zero at large distances $r$. Likewise, their Fourier transform $\hat{u}$ drops to zero for large wavenumbers $k$ and the transformation between $u$ and $\hat{u}$ via the corresponding radial Fourier integrals is unproblematic and rather straightforward to perform. However, when considering the inverse $\hat{u}^{-1}$ in eq 16, the decrease of $\hat{u}$ with $k$ (the magnitude of $\mathbf{k}$) results in an increase of $\hat{u}^{-1}$ with $k$. In turn, and given the rising values of the integrand in the Fourier integral with increasing $k$, this behavior renders the derivation of $u^{-1}$ through back Fourier transform quite challenging. By means of the intuitive potential smearing picture, the fundamental question may even arise whether it is in principle possible at all to transform nondelta functions by smearing to a single delta peak. The answer to this question can be found in the realm of the so-called implicit $\delta$-interactions already discussed in ref 14: there exist functions that have a very close but nonobvious connection to the delta function that becomes obvious only when we work in Fourier space, thus rendering such a smearing indeed possible. For the Yukawa potential of eq 10 or the Coulomb potential $u_c(\mathbf{r}) = \frac{\lambda_B'}{r}$ (which can also be considered as the limit of the Yukawa potential when $B_Y \to 0$), it is interesting to note that such an increase of $\hat{u}^{-1}$ with $k$ is captured by the Laplacian (acting on the delta function) with $u^{-1}$ then being specified by $u_c^{-1}(\mathbf{r}) = -\frac{1}{4\pi\lambda_B'}\nabla^2\delta(\mathbf{r})$. This nice property has already been exploited in a recent publication[15] to directly calculate $u^{-1}$ for advanced interatomic potentials.

**2.3. Multiconvolutions and Model Equivalence.** The adoption of a masking function implies a fundamental change in the nature of the original particle model, since

$$\langle\hat{\rho}|u|\hat{\rho}\rangle \neq \langle\Gamma*\hat{\rho}|u|\Gamma*\hat{\rho}\rangle \tag{17}$$

for $\Gamma(\mathbf{r}) \neq \delta(\mathbf{r})$ and general $u$. We have seen earlier that the field-theoretic Hamiltonian $\mathcal{H}'$ of the smeared model, eq 4, differs from the original Hamiltonian $\mathcal{H}$, eq 5, only as far as the functional argument of the reduced partition function $Q$ is concerned. That $Q$ is the only component of the field-theoretic model wherein the microscopic density appears has motivated a useful subscript shorthand notation below. Indeed, and given that the reduced partition function $Q$ is defined directly in terms of the $\langle w|\hat{\rho}\rangle$ leftover involving the microscopic density $\hat{\rho}$ from the particle-to-field transformation in the absence of any segment connectivity as

$$Q[iw]^n = \frac{1}{V^n}\int_{V^n} d^{3n}r\,\exp(-i\langle w|\hat{\rho}\rangle) \tag{18}$$

we can decorate $Q$ with a $\hat{\rho}$ subscript, namely, $Q[iw]_{\hat{\rho}} := Q[iw]$, so that for the single-convoluted microscopic density $\check{\rho}(\mathbf{r}) := [\Gamma * \hat{\rho}](\mathbf{r})$, we can write

$$\begin{aligned} Q[i\Gamma*w]^n &= \frac{1}{V^n}\int_{V^n} d^{3n}r\,\exp(-i\langle\Gamma*w|\hat{\rho}\rangle) \\ &= \frac{1}{V^n}\int_{V^n} d^{3n}r\,\exp(-i\langle w|\check{\rho}\rangle) \\ &=: Q[iw]^n_{\check{\rho}} \end{aligned} \tag{19}$$



https://doi.org/10.1021/acs.jpcb.2c06734
J. Phys. Chem. B 2022, 126, 10948−10954

where we have introduced the notation

$$Q[iw]_{\breve{\rho}} \coloneqq Q[i\Gamma * w] \tag{20}$$

to indicate the dependence of $Q$ on $\Gamma$ through $\breve{\rho}$. This motivates us to introduce a general (nondecorated) placeholder density $\rho$ associated with $Q$ for any (i.e., general) interatomic potential $u$. We also understand that

$$\langle w|u^{-1}|w\rangle \neq \langle w|\Gamma * u^{-1} * \Gamma|w\rangle \tag{21}$$

for $\Gamma(\mathbf{r}) \neq \delta(\mathbf{r})$ and general $u^{-1}$. Thus, it is advantageous to also label the (inverse) potential with an appropriate subscript so that, and with respect to inequality eq 21, the entire quantity

$$u_2^{-1}(\mathbf{r}) \coloneqq [\Gamma * u_1^{-1} * \Gamma](\mathbf{r}) \tag{22}$$

can be viewed as an effective convoluted inverse potential, further implying that

$$u_1(\mathbf{r}) = [\Gamma * u_2 * \Gamma](\mathbf{r}) \tag{23}$$

Let us now apply this idea to the particle-to-field transformation for two different models denoted as $(u_1, \rho_1)$ and $(u_2, \rho_2)$, respectively, with the understanding that potential $u_1$ is associated with a general microscopic density $\rho_1$, and potential $u_2$ is associated with a general microscopic density $\rho_2$. For the pair $(u_1, \rho_1)$, we can write

$$\int_{V^n} d^{3n}r \exp\left(-\frac{\beta}{2}\langle \rho_1|u_1|\rho_1\rangle\right) \propto \frac{\int \mathcal{D}w \exp\left(-\frac{1}{2\beta}\langle w|u_1^{-1}|w\rangle + n \ln Q[iw]_{\rho_1}\right)}{\int \mathcal{D}w \exp\left(-\frac{1}{2\beta}\langle w|u_1^{-1}|w\rangle\right)} \tag{24}$$

and, similarly, for the pair $(u_2, \rho_2)$, we can write

$$\int_{V^n} d^{3n}r \exp\left(-\frac{\beta}{2}\langle \rho_2|u_2|\rho_2\rangle\right) \propto \frac{\int \mathcal{D}w \exp\left(-\frac{1}{2\beta}\langle w|\Gamma * u_1^{-1} * \Gamma|w\rangle + n \ln Q[iw]_{\rho_2}\right)}{\int \mathcal{D}w \exp\left(-\frac{1}{2\beta}\langle w|\Gamma * u_1^{-1} * \Gamma|w\rangle\right)} \tag{25}$$

The last equation is compatible with the fact that the model described by $u_2^{-1}$ has been changed by another model involving the double convolution of $u_1^{-1}$ with the masking function $\Gamma$. Even more importantly, however, and in contrast to the GREM[3] case discussed above where the model was modified by smearing the microscopic density, now we have full freedom to choose the corresponding microscopic density field $\rho_2$ in relation to $\rho_1$ such that model equivalence is established. In particular, by requiring the statistical weights implied by the partition functions of eqs 24 and 25 to be equivalent, we find $\langle \Gamma * \rho_1|u_2|\Gamma * \rho_1\rangle \stackrel{!}{=} \langle \rho_2|u_2|\rho_2\rangle$ and thus

$$\rho_2(\mathbf{r}) \stackrel{!}{=} [\Gamma * \rho_1](\mathbf{r}) \tag{26}$$

Together with eqs 22 and 23, this connection between general microscopic densities can be used recursively to interconnect additional field descriptions, based on the particular choices of $(u_1, \rho_1)$ and $(u_2, \rho_2)$. From this perspective, one could also imagine introducing additional transformations, thus going from double convolutions to multiconvolutions.

To interpret the effect of transforming the field-theoretic model at the level of the particle-based description, let us consider first the case $\rho_1 = \hat{\rho}$ corresponding to point particles interacting via a physical pair potential $u_1$ for which the calculation of $u_1^{-1}$ as a standalone function may be difficult to accomplish due to a nondecaying behavior of $\hat{u}_1^{-1}$ in Fourier space, as we already explained above. We also consider the alternative case $\rho_2 = \breve{\rho}$ with $\breve{\rho}(\mathbf{r}) = [\Gamma * \hat{\rho}](\mathbf{r})$, with the understanding that we deal now with smeared particles interacting with each other through the pair potential $u_2$. In view of eq 23, it might appear that the specification of $u_2$ is as difficult to accomplish as the direct calculation of $u_1^{-1}$. However, through the principle of model equivalence, we require eqs 24 and 25 to provide equivalent complex probability weights as far as the calculation of statistical averages for the system properties under study is concerned. Then, the functional form of $u_2$ may remain only of hypothetical interest since problems in Fourier space arising from the ill-decaying behavior of $\hat{u}_1^{-1}$ can be circumvented in the case of $\hat{u}_2^{-1}$ by choosing a suitable masking function whose Fourier transform $\hat{\Gamma}$ decays appropriately fast compared to the slowly varying $\hat{u}_1^{-1}$. In this way, a standalone function $u_2^{-1}$ describing the inverse potential can be calculated, which can be used next to also study the original system (the one characterized by the interaction potential $u_1$ and the microscopic density $\rho_1$) through the corresponding field-theoretic Hamiltonian of eq 25, namely

$$\mathcal{H}_2[w] = \frac{1}{2\beta}\langle w|u_2^{-1}|w\rangle - n \ln Q[iw]_{\rho_2} \tag{27}$$

The proposed modeling scheme is highlighted in Figure 1 showing how the $(u_1, \rho_1)$ and $(u_2, \rho_2)$ pairs of FTS modeling blocks are linked together and how the principle of model equivalence helps compute $u_2^{-1}$. The $u_2^{-1}$ is connected to $u_1^{-1}$

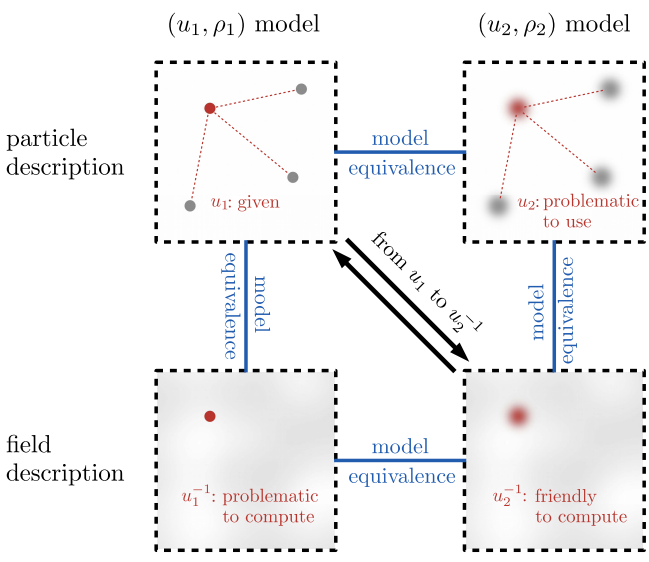


**Figure 1.** Schematic interpretation of the idea of a multiconvoluted inverse showing the passage from the $(u_1, \rho_1)$ to the $(u_2, \rho_2)$ pair of building blocks, their equivalence, and the final utilization of $u_2^{-1}$ to carry out efficient FTS calculations. Clouds on the upper and bottom right correspond to the smeared particles. A model involving the direct potentials $u_1$ and $u_2$ implies a particle description, whereas a model involving the inverse potentials $u_1^{-1}$ and $u_2^{-1}$ implies a field description.



https://doi.org/10.1021/acs.jpcb.2c06734
J. Phys. Chem. B 2022, 126, 10948−10954

Table 1. Correspondence between the Original GREM by Villet and Fredrickson[3] and the Convoluted GREM Proposed Here

| | original GREM | convoluted GREM |
|---|---|---|
| microscopic density | $\rho_1 = \Gamma * \hat{\rho}$ | $\rho_2 = \Gamma * \Gamma * \hat{\rho}$ |
| interaction potential | $u_1 = u_0\ \delta$ | $u_2$ not specified |
| inverse potential | $u_1^{-1} = u_0^{-1}\ \delta$ | $u_2^{-1} = \Gamma * u_1^{-1} * \Gamma$ |
| field-theoretic Hamiltonian | $\mathcal{H}_1 = \frac{1}{2\beta}\langle w\|u_1^{-1}\|w\rangle - n \ln Q[i\Gamma * w]$ | $\mathcal{H}_2 = \frac{1}{2\beta}\langle w\|\Gamma * u_1^{-1} * \Gamma\|w\rangle - n \ln Q[i\Gamma * \Gamma * w]$ |

through the masking function, which can be chosen at will, with two convolutions. It is this tremendous modeling freedom that multiconvoluted functions offer, which allows us to build realistic models in FTS that are more chemistry-specific and thus more physically relevant for the family of complex fluids that we wish to simulate, as discussed next with two examples.

## 3. RESULTS

**3.1. Multiconvoluted Edwards Model.** In the example of the GREM, a Gaussian masking function is used. As shown in Table 1, due to the simple form of the interactions, both $u_1$ and its inverse $u_1^{-1}$ can be analytically determined, but this is not so straightforward for $u_2$. Nevertheless, it is possible to specify the inverse $u_2^{-1}$ by requiring model equivalence. Moreover, in Table 1, the same $\Gamma$ has been used to denote both the masking function for the density and also for the passage from one model (the original) to the other (the convoluted one), which is not the case in general as one can imagine using two different $\Gamma$'s. To demonstrate then the equivalence of the original and of the convoluted models, we implemented the GREM in a fully fluctuating field calculation following ref 3. A physical quantity on which Villet and Fredrickson[3] put a special focus was the excess chemical potential defined in terms of the Helmholtz free energy as $\mu = \left.\frac{\partial A}{\partial n}\right|_{T,V}$ and which can be split into an ideal and an excess part, $\mu = \mu_{id} + \mu_{ex}$, with the excess part given by

$$\mu_{ex1,2} = -k_B T\langle \ln Q[iw]_{\rho_1,\rho_2}\rangle - \frac{n_m}{2}[\Gamma * u_1 * \Gamma](\mathbf{0}) \tag{28}$$

where $n_m$ is the number of monomers per chain. Based on this relation, we introduce a field-theoretic observable in connection with the excess chemical potential as

$$\tilde{\mu}_{1,2} = -\ln Q[iw]_{\rho_1,\rho_2} \tag{29}$$

such that

$$\beta\mu_{ex1,2} = \langle \tilde{\mu}_{1,2}\rangle - \frac{\beta n_m}{2}[\Gamma * u_1 * \Gamma](\mathbf{0}) \tag{30}$$

Following Villet and Fredrickson,[3] dimensionless units can be introduced and the chain propagators for continuous chains can be computed according to the pseudo-spectral algorithm[4] employing the improved scheme suggested by Ranjan, Qin, and Morse[19] for integration along the chain contour. For the $t$ integration of the complex Langevin (CL) equation, the limit method of ref 20 was used, a straightforward extension of the Euler−Maruyama (EM) method. Simulation results (instantaneous values) for the real part of the excess chemical potential-related observable $\tilde{\mu}$ from the two models are shown in Figure 2. In both cases, and starting from a (randomly chosen) initial state, the corresponding curves approach rapidly the equilibrium behavior where they are seen to fluctuate rapidly around the same asymptotic steady-state value. The equilibrium value is obtained as an ensemble average (the mean of the accumulated instantaneous values) in the asymptotic regime. For a consistent choice of $\Gamma$ (and only then), the two asymptotic values are observed to agree perfectly and are also in excellent agreement with the results of Villet and Fredrickson (Figure 2a in ref 3).

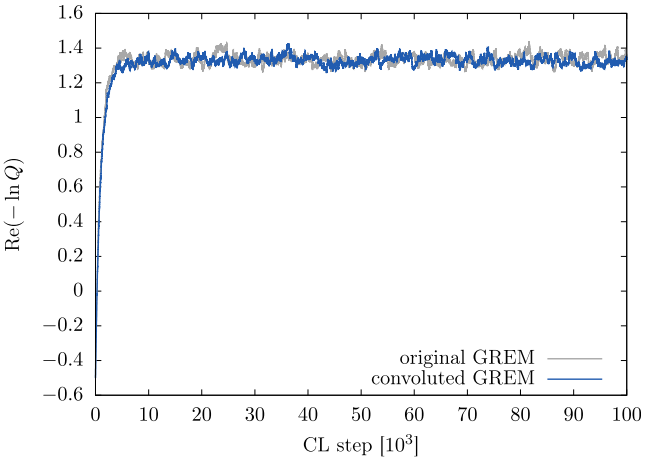


**Figure 2.** Comparison of the field-theoretic observable $\tilde{\mu}_1$ obtained from our implementation of the GREM following Villet and Fredrickson[3] against the observable $\tilde{\mu}_2$ of the novel alternative model proposed here.

**3.2. Yukawa Potential.** Of course, in the GREM example, the simple functional form of $u_1$ allows its inverse $u_1^{-1}$ to be determined rather straightforwardly. Thus, our basic intention (to apply the new methodology to derive an inverse $u_2^{-1}$ as a standalone function that exhibits the desired decaying behavior in Fourier space and which can then be computed numerically) is not fully revealed in this example. It is revealed, however, in the second example, that of the Yukawa potential, whose inverse, albeit not trivial to determine, is known.

For the Yukawa potential, $u_1 = u_Y$ as defined by eq 10. To calculate the inverse $u_2^{-1}$, it is useful to provide not only the Fourier transform $\hat{u}_Y$ of $u_Y$ itself, eq 11, but also the Fourier transform of the Gaussian masking function $\Gamma_G$ defined in ref 1, namely, $\hat{\Gamma}_G(\mathbf{k}) = \exp\left(-\frac{1}{2}a^2|\mathbf{k}|^2\right)$. With these Fourier transforms and the adjusted variance $\bar{\sigma}^2 := 2a^2$ of the Gaussian, the inverse $u_2^{-1}$ can be found from eq 22 and reads $\hat{u}_2^{-1}(\mathbf{k}) = \frac{1}{4\pi A_Y}(|\mathbf{k}|^2 + B_Y^2)\exp\left(-\frac{1}{2}\bar{\sigma}^2|\mathbf{k}|^2\right)$. The coupling of the first nondecaying interaction potential term to the second decaying exponential masking term is obvious. The presence of the exponential term makes the radial Fourier integral involving $\hat{u}_2^{-1}$ straightforward to solve for, which allows next to obtain the transform in the spatial domain



https://doi.org/10.1021/acs.jpcb.2c06734
J. Phys. Chem. B 2022, 126, 10948−10954

$$u_2^{-1}(\mathbf{r}) = -\frac{1}{4\pi A_Y}\left(\frac{|\mathbf{r}|^2}{\overline{\sigma}^4} - \frac{3}{\overline{\sigma}^2} - B_Y^2\right) \times \frac{1}{(2\pi\overline{\sigma}^2)^{3/2}} \exp\left(-\frac{|\mathbf{r}|^2}{2\overline{\sigma}^2}\right) \quad (31)$$

revealing a Gaussian contribution. Even more important, parts of the polynomial in parentheses can be replaced by the 3D Laplacian acting on the Gaussian such that the inverse can also be expressed as

$$u_2^{-1}(\mathbf{r}) = -\frac{1}{4\pi A_Y}(\nabla^2 - B_Y^2)\frac{1}{(2\pi\overline{\sigma}^2)^{3/2}} \exp\left(-\frac{|\mathbf{r}|^2}{2\overline{\sigma}^2}\right) \quad (32)$$

Then, and as in the GREM example and its alternative description as contrasted in Table 1, the inverse $u_2^{-1}$ may be used in an alternative FTS model defined, for instance, by $\mathcal{H}_2$ of eq 27.

Before we close this example, it is instructive to discuss the limiting behavior of $u_2^{-1}$. As it is apparent, the $u_2^{-1}$ approaches $u_1^{-1}$ in the limit that the masking function reduces to the Dirac delta function, i.e., in the limit of an infinitely narrow Gaussian function $\delta(\mathbf{r}) = \lim_{\overline{\sigma}\to 0} \frac{1}{(2\pi\overline{\sigma}^2)^{3/2}} \exp\left(-\frac{|\mathbf{r}|^2}{2\overline{\sigma}^2}\right)$. This representation of the Dirac delta function can be used to calculate the inverse of the Yukawa potential as a limiting case of eq 32

$$u_Y^{-1}(\mathbf{r}) = \lim_{\overline{\sigma}\to 0} u_2^{-1}(\mathbf{r}) = -\frac{1}{4\pi A_Y}(\nabla^2 - B_Y^2)\delta(\mathbf{r}) \quad (33)$$

the latter expression already being known from Edwards' seminal work.[2] Our work implies that, in the limit $\overline{\sigma} \to 0$, the model described by eqs 27 and 32 is mathematically identical to the model described by eqs 5 and 33. The case $\overline{\sigma} \to 0$ is also of interest in view of the Fourier transform $\hat{u}_2^{-1}$ and suggests that nondecaying functions in Fourier space are not problematic themselves, but it is the determination of the functional form of their inverse which is challenging. For nondecaying Fourier transforms, the latter cannot be accomplished by just solving the Fourier integral but requires appropriate representations such as, e.g., in terms of derivatives of the Dirac delta function, a path already followed in a recent contribution[15] to determine the inverse functional of the very important Morse interatomic potential.

A very interesting point about $u_2^{-1}$ is that, if we have computed it as a standalone function, the corresponding masking function needs not necessarily be a Gaussian (as long as it corrects for the ill-behaving increase of $\hat{u}_1^{-1}$ with $k$). This is quite an attractive feature of our methodology which could be exploited to overcome convergence problems in implementations of the CL method for generating new realizations of the fields since $u_2^{-1}$ appears directly in $\frac{\delta\mathcal{H}_2}{\delta w}$. With a judiciously chosen masking function, scalable and highly optimized field-update CL algorithms could thus be designed, characterized by improved stability and accuracy properties compared to existing codes.

## 4. CONCLUSIONS

We have presented a powerful model-building framework for the FTS of complex fluids based on the use of multiconvoluted inverse potentials and a principle of model equivalence that overcomes theoretical barriers associated with divergences of functional integrals and allows accommodating more chemistry-specific interactions in the microscopic model. In addition to opening new directions in the field, our work holds the promise of designing new CL sampling schemes characterized by improved accuracy, which would be an important development since it could further facilitate the use of the CL method in simulation studies of the fluctuating properties of complex polymer systems. In the present contribution, we used the new methodology to compute the excess chemical potential of a polymer chain and compare it with previous works. In the future, we plan to exploit the new method to address a variety of problems in soft matter, starting from the conformational properties of polymer solutions and melts, while retaining the connection of the microscopic model to the chemistry of the system.

## AUTHOR INFORMATION


### Corresponding Authors

**Alexander Weyman** − *Polymer Physics, Department of Materials, ETH Zurich, CH-8093 Zurich, Switzerland;* orcid.org/0000-0002-0659-3754; Email: alexander.weyman@mat.ethz.ch

**Vlasis G. Mavrantzas** − *Particle Technology Laboratory, Department of Mechanical and Process Engineering, ETH Zurich, CH-8092 Zurich, Switzerland; Department of Chemical Engineering, University of Patras & FORTH-ICE/HT, GR 26504 Patras, Greece;* orcid.org/0000-0003-3599-0676; Email: vlasios.mavrantzas@mat.ethz.ch

Complete contact information is available at: https://pubs.acs.org/10.1021/acs.jpcb.2c06734


### Notes

The authors declare no competing financial interest.

## ACKNOWLEDGMENTS

The authors are grateful to Hans Christian Öttinger for many stimulating discussions and for reading the manuscript prior to its submission for publication.

## REFERENCES


(1) Edwards, S. F. The statistical mechanics of polymers with excluded volume. *Proc. Phys. Soc.* **1965**, *85*, 613.

(2) Edwards, S. F. The theory of polymer solutions at intermediate concentration. *Proc. Phys. Soc.* **1966**, *88*, 265−280.

(3) Villet, M. C.; Fredrickson, G. H. Efficient field-theoretic simulation of polymer solutions. *J. Chem. Phys.* **2014**, *141*, No. 224115.

(4) Fredrickson, G. H. *The Equilibrium Theory of Inhomogeneous Polymers*; Oxford University Press, 2006.

(5) Delaney, K. T.; Fredrickson, G. H. Recent Developments in Fully Fluctuating Field-Theoretic Simulations of Polymer Melts and Solutions. *J. Phys. Chem. B* **2016**, *120*, 7615−7634.

(6) Sherck, N.; Shen, K.; Nguyen, M.; Yoo, B.; Köhler, S.; Speros, J. C.; Delaney, K. T.; Shell, M. S.; Fredrickson, G. H. Molecularly Informed Field Theories from Bottom-up Coarse-Graining. *ACS Macro Lett.* **2021**, *10*, 576−583.

(7) Matsen, M. W. Field theoretic approach for block polymer melts: SCFT and FTS. *J. Chem. Phys.* **2020**, *152*, No. 110901.

(8) Wang, Z.-G. Fluctuation in electrolyte solutions: The self energy. *Phys. Rev. E* **2010**, *81*, No. 021501.

(9) Prakash, J. R.; Öttinger, H. C. Viscometric functions for a dilute solution of polymers in a good solvent. *Macromolecules* **1999**, *32*, 2028−2043.
(10) Hömberg, M.; Müller, M. Main phase transition in lipid bilayers: Phase coexistence and line tension in a soft, solvent-free, coarse-grained model. *J. Chem. Phys.* **2010**, *132*, No. 155104.
(11) Müller, M. Studying Amphiphilic Self-assembly with Soft Coarse-Grained Models. *J. Stat. Phys.* **2011**, *145*, 967−1016.
(12) Laradji, M.; Guo, H.; Zuckermann, M. J. Off-lattice Monte Carlo simulation of polymer brushes in good solvents. *Phys. Rev. E* **1994**, *49*, 3199−3206.
(13) Miao, L.; Guo, H.; Zuckermann, M. J. Conformation of Polymer Brushes under Shear: Chain Tilting and Stretching. *Macromolecules* **1996**, *29*, 2289−2297.
(14) Weyman, A.; Mavrantzas, V. G.; Öttinger, H. C. Field-theoretic simulations beyond $\delta$-interactions: Overcoming the inverse potential problem in auxiliary field models. *J. Chem. Phys.* **2021**, *155*, No. 024106.
(15) Weyman, A.; Mavrantzas, V. G.; Öttinger, H. C. Direct calculation of the functional inverse of realistic interatomic potentials in field-theoretic simulations. *J. Chem. Phys.* **2022**, *156*, No. 224115.
(16) Villet, M. C. Advanced Computational Field Theory Methods for Fluctuating Polymer Solutions. Ph.D. Thesis, University of California, Santa Barbara, 2012.
(17) Koski, J.; Chao, H.; Riggleman, R. A. Field theoretic simulations of polymer nanocomposites. *J. Chem. Phys.* **2013**, *139*, No. 244911.
(18) Likos, C. N. Effective interactions in soft condensed matter physics. *Phys. Rep.* **2001**, *348*, 267−439.
(19) Ranjan, A.; Qin, J.; Morse, D. C. Linear Response and Stability of Ordered Phases of Block Copolymer Melts. *Macromolecules* **2008**, *41*, 942−954.
(20) Leimkuhler, B.; Matthews, C.; Tretyakov, M. On the long-time integration of stochastic gradient systems. *Proc. R. Soc. A* **2014**, *470*, No. 20140120.


https://doi.org/10.1021/acs.jpcb.2c06734
*J. Phys. Chem. B* 2022, 126, 10948−10954